The role of zinc dopant and the temperature effect on the controlled growth of InN nanorods in metal–organic chemical vapor deposition system

Huaping Song,* Yan Guo, Anli Yang, Hongyuan Wei, Xiaoqing Xu, Jianming Liu, Shaoyan Yang, Xianglin Liu,* Qinsheng Zhu* and Zhanguo Wang

Received 29th March 2010, Accepted 26th May 2010
DOI: 10.1039/c0ce00046a

Vertically well-aligned InN nanorods have been synthesized successfully by introducing diethylzinc (DEZn) into metal–organic chemical vapor deposition system. X-Ray diffraction and transmission electron microscopy measurements show that InN nanorods are single-crystalline and Zn-doped. In-depth studies indicate that DEZn inhibits the InN growth along *m*-plane and further leads to the self-formation indium droplets acting as catalyst. The whole growth process of InN nanorods is a combined result of the restriction effect from DEZn and catalytic effect from indium droplets. Also, the temperature effect on the growth has been studied intensively. Our research on the controlled growth of high-quality InN nanorods is very important for InN-based optoelectronic and electronic nano-devices.

1. Introduction

Semiconductor nanostructures have received steadily growing interests due to their peculiar properties and applications superior to their bulk materials.[1–3] In the past decades, many efforts were focused on the control of the size and morphology of semiconductors nanostructures.[4–7] The method with foreign element catalytic agent (FECA) has been widely applied to mediate nanostructures growth.[3,8,9] In general, the first step in this method is to arrange metal particles on the substrate surface, and the next step is to insert this substrate into the growth chamber.[10] The diameters of the nanowires are decided by the size of the metallic seed particles and the driving force for crystallization is supersaturation within the droplets.[10–12] For InN nanostructures growth, noble metals are also used as FECA.[13]

However, there are some limits or disadvantages when FECA are used; for example, the selection of catalyst species and catalyst element contamination. Also, noble metals are not feasible to remove from the as-grown nanostructures before employing them to fabricate devices. Self-catalyzed growth method has been proven to be another effective method to grow semiconductors nanostructures.[14–16] Differing from FECA, self-formed liquid droplets act as the catalyst and mediate the growth of nanostructures during the self-catalyzed growth process. To acquire desired morphology of nanostructures, special-designed growth conditions or processes are needed, and it is a big issue to study the control growth of nanostructures.[14,17,18]

In this work, we report on the growth of vertically well-aligned Zn-doped InN nanorods under different growth conditions in metal–organic chemical vapor deposition (MOCVD) system. The role of DEZn in the growth of nanorods is studied intensively. Our research shows that the successful growth of InN nanorods is a combined result of diethylzinc (DEZn) and metal indium droplets. Basing on the understanding of the key growth processes, we also investigate the temperature effects on the growth of InN nanorods.

Key Laboratory of Semiconductor Materials Science, Institute of Semiconductors, Beijing, 100083, China. E-mail: songhp@semi.ac.cn; xlliu@semi.ac.cn; qszhu@semi.ac.cn; Fax: +86-10-82304576; Tel: +86-10-82304968

2. Experimental

All the samples in our experiments were synthesized in a home-made MOCVD system. *C*-plane sapphires were used as substrates. Trimethylindium (TMIn) and NH_3 were used as precursors, and DEZn was dopant. High purity N_2 was used as carrier gas. Before growth, the sapphire wafer was heated under a hydrogen flow at 1050 °C for 20 min to remove the adsorbed water molecules and activate sapphire surface. Subsequently, sapphire wafer was nitridized for 3 min under a mixed gas of H_2 and NH_3 with a flow rate of 3 SLM (standard litre per minute), respectively. Before the growth of InN nanorods, a thin low-temperature (550 °C) GaN buffer layer was initially grown for 3.5 min (trimethylgallium: 25 μmol min^{-1}, pressure: 50 Torr). Then the growth temperature was set to the desired value, and InN nanorods were grown at atmospheric pressure. Except for the growth temperatures (T_g) and the flow rates of TMIn and DEZn (as shown in Table 1), other growth conditions were the same as that described in our previous research.[19] Finally, the TMIn and DEZn currents were cut off and the furnace was cooled down to the room temperature. Ammonia was

Table 1 Growth conditions and morphology properties of the products. H denotes the height of the highest rod in the sample, and t is the thickness of InN film at the bottom of nanorods

Sample	T_g °C	TMIn μmol min^{-1}	DEZn μmol min^{-1}	H μm	t nm	Time min
A1	520	16	0.7	4.6	275	40
A2	550	16	0.7	4.2	300	40
A3	580	16	0.7	3.8	410	40
A4	600	16	0.7	—	350	40
A5	550	8	0.7	2.2	220	40
A6	580	16	0	—	400	40

maintained during cooling down in order to prevent the decomposition of InN.

The products were characterized using the High-Resolution X-ray diffraction (HR-XRD) apparatus at Beijing Synchrotron Radiation Facility (BSRF). The incident X-ray beam is monochromized to 0.154791 nm by a Si (111) monocrystal. The morphology and size of the products were investigated by field-emission scanning electron microscopy (FE-SEM: Hitachi S-4800), and the crystallinity of InN nanorods was examined by high-resolution transmission electron microscopy (HR-TEM: JEM 2010, 200 KV) attached to an energy-dispersive X-ray spectrometer.

3. Results and discussions

3.1 The growth results

Fig. 1 shows the HR-XRD pattern of the sample A1. Peak position is indicated on the each corresponding diffraction. The peaks at 31.42° and 65.52° correspond to wurtzite (*w*-) InN (002) and (004) respectively, which is in agreement with the data on the Joint Committee of Powder Diffraction Standards (JCPDS) card (79-2498: *w*-InN). Also, the diffractions from low temperature GaN buffer layer wurtzite (*w*-) GaN (002) and (004) are observed at 34.48° and 72.66° (JCPDS: 76-0703, *w*-GaN). And the diffractions at 32.96° and 69.1° indicate the existence of metal indium (JCPDS: 85-1409), corresponding to tetragonal In (101) and (202), respectively. Due to the using of an attenuator, the diffraction from sapphire (006) can be seen at 41.72° with the magnification of 20 times. No other diffraction peak is determined, showing the as-synthesized InN products are single-crystalline.

Typical FE-SEM images of the products are shown in Fig. 2. In an appropriate temperature range (520∼580 °C), vertical aligned InN nanorods were synthesized successfully [Fig. 2(a)–(c)]. However, no InN nanorods were grown when the T_g arrived at 600 °C (Fig. 2(d)). We note that the InN nanorods become more tapering as the T_g increases. To examine the crystal structure of tapering InN nanorods, the product was scraped off from sample A2 and dispersed onto copper grids with an amorphous carbon film for TEM measurement by JEM 2010.

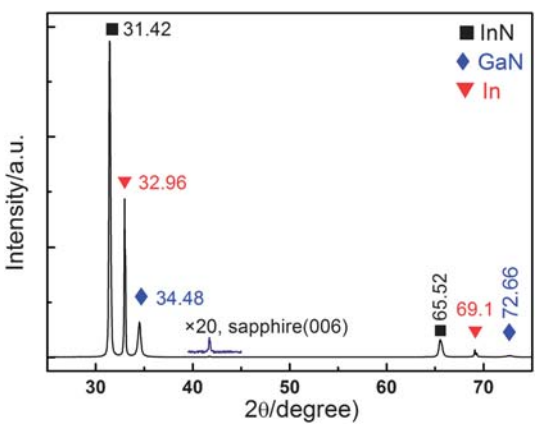

Fig. 1 XRD pattern of the sample A1. Miller indices and peak positions are indicated on the corresponding diffraction peaks.

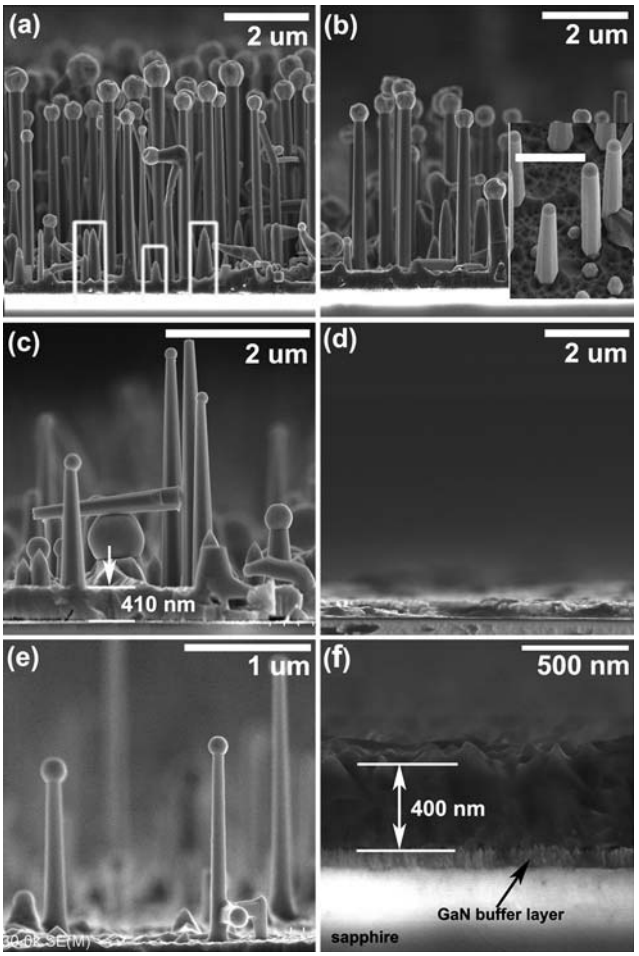

Fig. 2 Typical FE-SEM images of products. (a–e) Side-view images of A1–A5, respectively. (f) Side-view image of A6. The growth conditions of A1–A6 are shown in Table 1. Inset in Fig. 2(b) is titled 20° image of the area around the bottom of nanorods, which shows the InN nucleation on the surface. The scale is 1 μm.

Fig. 3 shows the TEM measurements of a tapering InN nanorod from A2. Although tapered, the sidewall of InN nanorod is quite smooth like the no-tapering InN nanorods.[19] Fig. 3(b) is the selected area electron diffraction (SAED) pattern on the tip of nanorod. According to the effective camera length (80 cm) and operating voltage (200 KV), the SAED pattern is labeled just below the diffraction spot itself. It shows that the SAED pattern was taken along the [110] zone axis of wurtzite InN, and the tapering InN nanorod is good single-crystalline.

Fig. 3(c) is the energy-dispersive X-ray spectroscopy (EDXS) taken from the place labeled in Fig. 3(a) and the inset is the corresponding chemical composition. It shows that the InN nanorod is Zn-doped. These TEM results show that the tapering InN nanorod has the same crystalline phase and growth direction with the nanorod with uniform diameter that was previously reported.

3.2 The role of dopant

To study the role of DEZn in the growth of InN nanorods, the general growth model for vapor-liquid-solid (VLS) growth

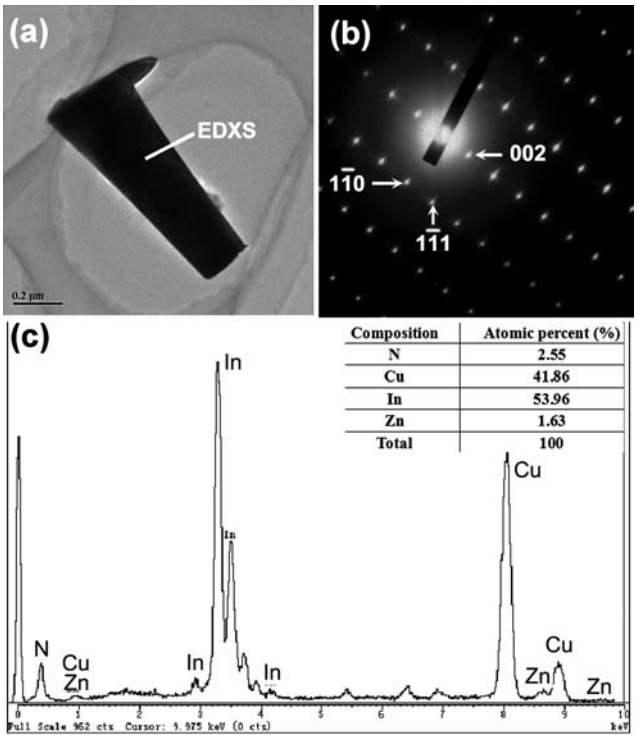

Fig. 3 HR-TEM results of a tapering InN nanorod. (a) Low magnification TEM image, (b) SAED pattern taken along the [110] zone axis, and (c) EDXS spectrum measured at the marked place in (a). Inset is the chemical composition of InN nanorod determined by EDXS.

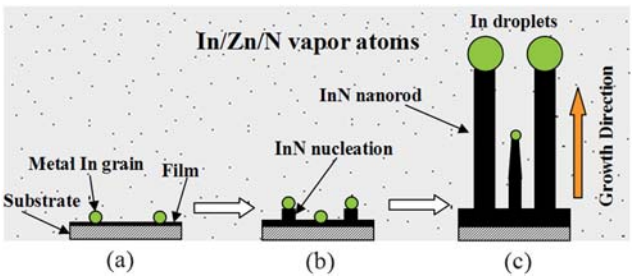

Fig. 4 Schematic illustration of Zn-doped InN nanorods growth process.

should be outlined first. As shown in Fig. 4, step (a), (b) and (c) present three different growth stages in VLS growth, respectively. In step (a), tiny indium grains are formed at the edges or corners of the surface. Due to the low melting point of indium (156.6 °C), these indium grains are liquid during the InN growth. Under the catalyst effect of indium, InN nuclei with indium grains grow faster and then create nucleation centers for InN nanorods growth [step (b)], this can be confirmed in the inset of Fig. 2(b). After dipping in dilute hydrochloric acid (HCl), indium droplets are removed and InN nuclei can be observed clearly. These nucleation centers act as seeds for InN nanorods growth. As the growth process goes on, InN nanorods are synthesized and tiny indium grains evolved into droplets [step (c)].

However, the growth model described above can not explain the growth of InN nanorods in our experiments fully. We note that samples A1–A3 were grown under normal growth conditions for InN film, except for the introducing of DEZn. As shown in Fig. 2(f), only InN film can be grown without introducing DEZn at the same growth condition. To our best knowledge, our result is the first report on the dopant-modulated growth of InN nanorods. So, it is very important for us to make certain the reason why the introducing of DEZn can lead to the growth of InN nanorods. To settle this question, two other representative experiments were carried out:

One is the growth of InN under the pure catalyst effect of indium nano-particles without DEZn (sample A7). After the nitridation in the mixed gas of H_2 and NH_3, the temperature was set at 500 °C and the TMIn flow (16 μmol min^{-1}) was introduced for 180 s. Fig. 5(a) shows the typical FE-SEM image of indium particles with most diameters ranging from 50 to 200 nm, and Fig. 5(b) illustrates the HR-XRD result of the sapphire substrate coating with indium particles. Similar to the XRD pattern in the as-grown InN nanorods, the diffraction peaks at 33.00° and 69.25° correspond to In(101) and In(202), respectively. Without interrupting the TMIn flow after predepositing indium particles, the ammonia flow of 3 SLM was introduced for InN growth at 580 °C lasting for 40 min. Fig. 5(c) shows the cross-section FE-SEM image of the growth result. It clearly shows that no InN nanorods were formed under the catalyst effect of pure indium particles, without introducing DEZn.

Another experiment is the observation on the growth of InN nanorod without DEZn (sample A8). Firstly, 30 min growth of Zn-doped InN nanorods was performed. The growth condition was the same as sample A1 [shown in Fig. 2(a)]; and then DEZn flow was cut off, but other growth conditions remained unchanged, this growth stage lasted for 6 min. The

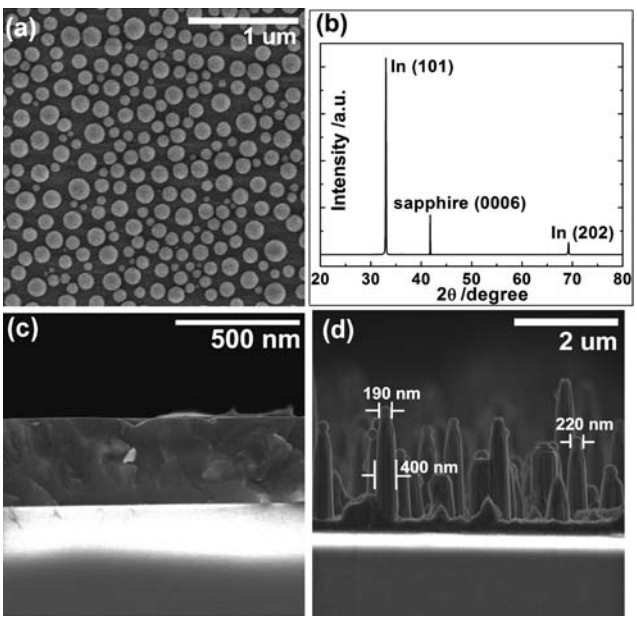

Fig. 5 (a) Bird-view FE-SEM image of indium particles formed on *c*-sapphire after 180 *s* predepositing (TMIn: 16 μmol min^{-1}); (b) XRD result of the substrate coating with indium particles; Side-view FE-SEM image of as-synthesized product (c) A7: under the pure catalyst effect of indium particles and (d) A8: 30-min-growth InN nanorods and then 6-min-growth without DEZn.

corresponding cross-section FE-SEM image of this sample is shown in Fig. 5(d). The characters as follows makes it is very different from sample A1: I) In our experiment, the height of nanorods is nearly proportional to the growth time if the growth conditions remain unchanged. However, the highest InN nanorods in A8 is only about 3 μm. It seems that the later 6 min growth without DEZn did not increase the height of nanorods; II) the diameters of indium droplets on the top of nanorods (less than 250 nm) is much smaller than these in Fig. 2(a); III) the diameters of InN nanorods here (~400 nm) are much larger than these in Fig. 2(a). This is the key point leading us to understand the role of DEZn in the growth of InN nanorods. It means that the DEZn can inhibit the growth of InN along *m*-plane, and the diameters of InN nanorods will increase without the restriction from DEZn.

It is important to note that the growth temperatures for Fig. 2(c) and Fig. 2(f) are all 580 °C, and the thickness of InN film at the bottom of nanorods in Fig. 2(c) is comparable with that of InN film in Fig. 2(f). This suggests that the growth of InN along *c*-axis is hardly changed by zinc doping.

Supposing that the axial growth (along *c*-axis) is nearly unchanged, but the lateral growth (along *m*-plane) is inhibited by zinc doping, the growth of Zn-doped InN nanorods can be understood fully. By introducing DEZn, the 2-dimensional (2D) growth of InN nuclei is restricted, and the superfluous indium atoms will lead to the formation of metal indium droplets. Under the catalyst effect of metal indium droplets, InN nuclei with indium droplets evolve to InN nanorods eventually. Due to the restricted lateral growth, the diameters of InN nanorods rely more on the radii of indium droplets, not on the growth time. So, the successful growth of InN nanorods is a combined result of diethylzinc (DEZn) and metal indium droplets.

The influence on the growth process of GaN from doping has been reported by Stamplecoskie.[20] In their work, GaN nanowires had a specific cross section as a function of the dopant precursor concentration in the reaction mixture: from pure GaN nanowires with hexagonal cross sections to triangular and eventually rectangular nanowires. They also found not only $MnCl_2$, $CoCl_2$ and $CrCl_2$ but also their transition-metal acetates can play such a role in the growth. In Wu's recent work, the diameter of ZnO nanorods was affected by Mn^{2+} doping concentration in the aqueous solution.[21] Also, the previous study on the growth of $Zn_{1-x}Mg_xO$ nanorods in our group has shown solid evidence that the dopant agent can change the growth mode in MOCVD.[22] Our experiments show that DEZn can modulate the growth of InN. Our previous research on the nonhomogeneous distribution of Zn in InN nanorod showed that Zn atoms can be adsorbed on the *m*-plane of InN and diffuse into the nanorod. The adsorbed Zn atoms at *m*-plane may affect the diffusion or adsorption of indium atoms at *m*-plane, so the lateral growth is restricted by Zn doping, nevertheless the reason why the Zn on the sidewall restricts the lateral growth should be studied more deeply.

3.3 The temperature effects

Now, we focus on the temperature effects on the growth of InN nanorods. These studies not only enable in-depth understanding of the growth process, but also allow us to control the morphology of nanorods. The film thickness (t) and the height of nanorods (H) are shown in Table 1. It should be noted that the height of InN nanorod in each sample is not uniform, so the height of the highest InN nanorod was adopted because the InN nuclei can be formed at different growth stages and the highest InN nanorod is more representative. As shown in Fig. 6(a), the thickness of InN film at the bottom of nanorods (A1–A3) increased as T_g rises. When T_g arrived at 600 °C, the thickness of the InN film decreased and the growth of nanorods was failed. As we know, ammonia pyrolysis will be enhanced at a higher temperature. This will result in a higher growth rate of InN. This relation between the growth rate of InN film at the bottom of InN nanorods and growth temperature coincides with Yamamoto's result very well.[23] If the same relation governs the growth of nanorods, the height of nanorods will increase as T_g rises (below 600 °C). To our surprise, the height of A1–A3 decreases as the temperature rises, which is clearly shown in Table 1 and Fig. 2(a)–(c).

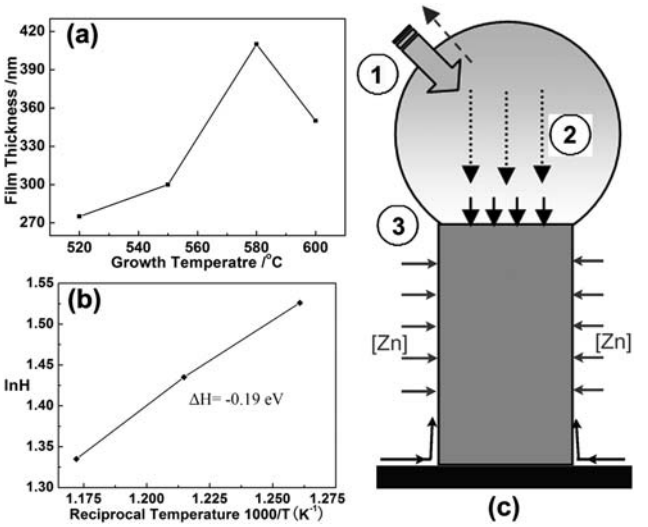

Fig. 6 (a) The thickness of InN film *versus* growth temperature; (b) Arrhenius plot of the height of nanorods *versus* reciprocal temperature; (c) Schematic illustration of three key processes in the growth of InN nanorods. [Zn] pointing at the sidewall of nanorod means the absorbed zinc atoms inhibit the growth along the sidewall, and the curve with double arrows denotes the diffusion from base layer through the sidewall.

As mentioned before, the driving force for crystallization in VLS growth is supersaturation within the droplets. The indium supply is always abundant for the growth of InN nanorods at the liquid–solid (LS) interface as long as the indium droplets are on the top of nanorods. Considering the transport of nitrogen atoms, there are three key processes which can affect the growth rate of InN nanorods, as shown in Fig. 6(c). Step 1 is the absorption and desorption of nitrogen at the vapor–liquid (VL) interface; step 2 is the transfer of nitrogen under the concentration gradient from VL to LS interface; and step 3 denotes the nitrogen atoms arrive at the LS interface and InN nanorod is formed here. Under the catalysis effect of indium droplets, the supply of nitrogen at the VL interface is sufficient. It should be noted that the elementary gas has a low solubility in metallic liquid. So the supply of nitrogen at the LS interface which is determined by step 2 is the bottleneck for nanorods growth,

although the increase of T_g will enhance step 1 and step 3. According to Clausius–Clapeyron equation, we can write the relation between the solubility of nitrogen in metal indium droplet and T_g as:

$$n_c \propto \exp\left(-\frac{\Delta H}{RT_g}\right) \quad (1)$$

where n_c is the solubility of nitrogen in metal indium droplet, ΔH is the reaction enthalpy of the dissolution and R is the universal gas constant (8.314 J K^{-1} mol^{-1}). At a certain temperature, the reaction rate at the LS interface has the relation as follows:

$$k \propto [In].[N] \quad (2)$$

where k is the reaction rate at the LS interface, [In] and [N] denotes the concentration of indium and nitrogen at the LS interface, respectively. We can identify [N] with n_c due to the small size of indium droplet. So, the relation between the reaction rate or H (height of nanorods) and T_g can be treated approximately as:

$$k \propto \exp\left(-\frac{\Delta H}{RT_g}\right) \text{ or } H \propto \exp\left(-\frac{\Delta H}{RT_g}\right) \quad (3)$$

The height of nanorods is plotted against the reciprocal temperature in Fig. 6(b). Within the appropriate growth temperature range for nanorods (500–580 °C), the Arrhenius relation is satisfied, with $\Delta H = -0.19$ eV (-18 KJ.mol^{-1}). This shows that the growth rate of nanorods is controlled by the solubility of nitrogen in a metal indium droplet in our experiments, not the pyrolysis rate of NH_3.

The density of nanorods is also affected by growth temperature. Fig. 2(a)–(c) clearly shows that the density of nanorods decreases as T_g increases. The pyrolysis rate of NH_3 is enhanced at higher temperature and the effective V/III ratio is higher. According to previous research on the growth of InN,[24,25] the formation of indium droplets will be suppressed under a high V/III ratio; also, Stranski-Krastanov (SK) mode is preferred and the highly faceted rough surfaces will be formed. Consequently, the density of nanorods is reduced at a higher temperature due to the decreased formation of indium droplets. This explanation can be proved by sample A5 [Fig. 2(e)]. By reducing the TMIn flow rate to 8 μmol min^{-1}, the V/III ratio could be directly changed. The nanorods in sample A5 (550 °C) is much sparser than sample A2 (550 °C) and even sparser than sample A3 (580 °C). It strongly evidences that the density of nanorods is controlled by the effective V/III ratio, including the growth temperature and V/III ratio.

Most of InN nanorods have metal indium droplets on them, whereas some of them do not, as shown in the white box in Fig. 2(a). These nanorods without droplets have the cone shapes, and they are always shorter. We call them nanocones. We should distinguish these nanocones from the tapering nanorods. Different from the nanocones, the diameter of tapering nanorod shrinks gradually from the bottom to the top, but the indium droplets remain on their top. We suggest the formation of these nanocones is attributed to the variation of growth condition occurred during their growths. On principle, the nucleation centers can be formed at the initial growth stage or sometime later [as shown in the inset of Fig. 2(b)]. The droplets are consumed during the nanorods growth and get supply from the vapor phase. Unavoidably, the growth rate of some later formed InN nanorods will fall behind the higher nanorods because the lower nanorods get less supply from the growth ambiance, like the shrub in the forest. So the size of indium droplets on them shrinks when the consumption rate is larger than the supply. Considering the effect of additional pressure on the saturated vapour pressure of curved liquid surface, the smaller spherical liquid droplet has a larger vapour pressure on the surface, this will lead to a growing difficulty with the source supply and then an accelerated shrink of the size of indium droplets until the exhaustion of indium droplets. This is the reason why the nanocones often have rapid-shrinking tips, comparing with the tapering nanorods has a gradually-decreasing diameters.

Two supply paths are often mentioned to describe VLS growth: the direct supply from the gas ambiance and the diffusion from the base layer through the sidewall. The latter is indicated by the curve with double arrows in Fig. 6(c), and we also notice that it may play an important role during the VLS growth.[26] However, the growth of nanorod in our experiments is attributed to the former. The following reasons below prove our opinion: (1) the diffusion of indium atoms will decrease when V/III ratio is increased.[25] In our experiments, the V/III ratio is high. And the rough surface of bottom most InN film indicates the short diffusion length of indium atoms during the growth; (2) If the axial growth of nanorod is controlled by the diffusion through sidewall, the height of nanorod will be limited by the diffusion length of atoms, just like the widely reported works.[26,27] The height of nanorod in our sample exceed 4 μm. We have also grown ~8μm InN nanorods (figure not shown here). However, no limited growth was observed in our experiments; (3) As described before, InN nanocones will be formed when the density of nanorods is very high. If the diffusion through the sidewall always plays an important role during the whole growth, nanocones will not be formed while the growth of normal nanorods continues. Due to the extremely low saturated vapor pressure of liquid indium, it is very easy for indium droplets to get the supply from the gas ambient. So, the supply from the gas ambient dominates the growth of nanorods in our case.

These studies show that the effective V/III ratio, the growth temperature, and the DEZn flow are important for the InN nanorods growth. If the uniform-height nanorods are wanted, the control of initial nucleation is crucial, also the growth temperature, pressure in the growth chamber and chemical composition in growth ambiance might be adjusted carefully because they play important effect on the droplet stability. The controlled growth of vertical-aligned InN nanorods with desired morphology is very important for applications such as bio-/gas sensors, optoelectronics devices, solar cell and so on.

4. Conclusion

In summary, the role of DEZn in the growth of InN nanorods has been studied intensively. The formation of InN nanorods is a combined result of DEZn and metal indium droplets: the introducing of DEZn leads to the formation of indium droplets and inhibits the growth of InN along *m*-plane; indium droplets catalyze the growth of InN nanorods and control the diameter and shape of InN nanorods. Our studies also show that the

density and growth rate of InN nanorods depend heavily on the growth temperature. The researches in this paper help us to better understand the growth processes and controllable growth of InN nanorods in metal–organic chemical vapor deposition system.

Acknowledgements

This work was supported by the National Science Foundation of China (60976008 and 60776015), the Special Funds for Major State Basic Research Project (973 program) of China (2006CB604907), and the 863 High Technology R&D Program of China (2007AA03Z402 and 2007AA03Z451). The authors express their appreciations to Prof. Yongliang Li (Analytical and Testing Center, Beijing Normal University) for FE-SEM measurements, to Dr Tieying Yang and Prof. Huanhua Wang (Beijing Synchrotron Radiation Facility, Institute of High Energy Physics, Chinese Academy of Sciences) for XRD measurements and helpful discussions.

Reference

1 W. Lu and C. M. Lieber, *J. Phys. D: Appl. Phys.*, 2006, **39**, R387.
2 P. D. Yang, *MRS Bull.*, 2005, **30**, 85.
3 X. Duan, Y. Huang, Y. Cui, J. Wang and C. M. Lieber, *Nature*, 2001, **409**, 66.
4 C. K. Kuo, C. W. Hsu, C. T. Wu, Z. H. Lan, C. Y. Mou, C. C. Chen, Y. J. Yang, L. C. Chen and K. H. Chen, *Nanotechnology*, 2006, **17**, S332.
5 P. V. Radovanovic, C. J. Barrelet, S. Gradečak, F. Qian and C. M. Lieber, *Nano Lett.*, 2005, **5**, 1407.
6 S. A. Dayeh, E. T. Yu and D. Wang, *Nano Lett.*, 2007, **7**, 2486.
7 H. J. Fan, P. Werner and M. Zacharias, *Small*, 2006, **2**, 700.
8 E. P. A. M. Bakkers and M. A. Verheijen, *J. Am. Chem. Soc.*, 2003, **125**, 3440.
9 H. S. Chung, Y. Jung, T. J. Zimmerman, S. Lee, J. W. Kim, S. H. Lee, S. C. Kim, K. H. Oh and R. Agarwal, *Nano Lett.*, 2008, **8**, 1328.
10 J. Johansson, L. S. Karlssom, K. A. Dick, J. Bolinssom, B. A. Wacaser, K. Deppert and L. Samuelson, *Cryst. Growth Des.*, 2009, **9**, 766.
11 A. I. Perssom, M. W. Larsson, S. Stenström, B. J. Ohlsson, L. Samuelson and L. R. Wallenberg, *Nat. Mater.*, 2004, **3**, 677.
12 S. Noor Mohammad, *Nano Lett.*, 2008, **8**, 1532.
13 C. H. Liang, L. C. Chen, J. S. Hwang, K. H. Chen, Y. T. Hung and Y. F. Chen, *Appl. Phys. Lett.*, 2002, **81**, 22.
14 M. Zha, D. Calestani, A. Zappettini, R. Mosca, M. Mazzera, L. Lazzarini and L. Zanotti, *Nanotechnology*, 2008, **19**, 325603.
15 M. He, A. Motayed and S. Noor Mohammad, *J. Chem. Phys.*, 2007, **126**, 064704.
16 H. F. Li, Y. H. Huang, Y. Zhang, J. J. Qi, X. Q. Yan, Q. Zhang and J. Wang, *Cryst. Growth Des.*, 2009, **9**, 1863.
17 C. C. Wu, D. S. Wuu, P. R. Lin, T. N. Chen and R. H. Horng, *Cryst. Growth Des.*, 2009, **9**, 4555.
18 R. L. Woo, L. Gao, N. Goel, M. K. Hudait, K. L. Wang, S. Kodambaka and R. F. Hicks, *Nano Lett.*, 2009, **9**, 2207.
19 H. P. Song, A. L. Yang, R. Q. Zhang, Y. Guo, H. Y. Wei, G. L. Zheng, S. Y. Yang, X. L. Liu, Q. S. Zhu and Z. G. Wang, *Cryst. Growth Des.*, 2009, **9**, 3292.
20 K. G. Stamplecoskie, L. Ju, S. S. Farvid and P. V. Radovanovic, *Nano Lett.*, 2008, **8**, 2674.
21 D. W. Wu, Z. B. Huang, G. F. Yin, Y. D. Yao, X. M. Liao, D. Han, X. Huang and J. W. Gu, *CrystEngComm*, 2010, **12**, 192.
22 A. L. Yang, H. Y. Wei, X. L. Liu, H. P. Song, G. L. Zheng, Y. Guo, C. M. Jiao, S. Y. Yang, Q. S. Zhu and Z. G. Wang, *J. Cryst. Growth*, 2009, **311**, 278.
23 A. Yamamoto, Y. Murakami, K. Koide, M. Adachi and A. Hashimoto, *Phys. Status Solidi B*, 2001, **228**, 5.
24 Y. F. Ng, Y. G. Cao, M. H. Xie, X. L. Wang and S. Y. Tong, *Appl. Phys. Lett.*, 2002, **81**, 3960.
25 G. Koblmüller, C. S. Galliant, S. Bernardis and J. S. Speck, *Appl. Phys. Lett.*, 2006, **89**, 071902.
26 V. G. Dubrovskii, G. E. Cirlin, I. P. Soshnikov, A. A. Tonkikh, N. V. Sibirev, Yu. B. Samsonenko and V. M. Ustinov, *Phys. Rev. B: Condens. Matter Mater. Phys.*, 2005, **71**, 205325.
27 J. C. Harmand, M. Tchernycheva, G. Patriarche, L. Travers, F. Glas and G. Cirlin, *J. Cryst. Growth*, 2007, **301–302**, 853.